How to cite: Angew. Chem. Int. Ed. 2023, e202306188
doi.org/10.1002/anie.202306188

Sustainable Polymers Hot Paper

Closed-Loop Recycling of Vinylogous Urethane Vitrimers

Youwei Ma, Xuesong Jiang, Zixing Shi, José Augusto Berrocal,* and Christoph Weder**

Abstract: Devising energy-efficient strategies for the depolymerization of plastics and the recovery of their structural components in high yield and purity is key to a circular plastics economy. Here, we report a case study in which we demonstrate that vinylogous urethane (**VU**) vitrimers synthesized from bis-polyethylene glycol acetoacetates (**aPEG**) and tris(2-aminoethyl)amine can be degraded by water at moderate temperature with almost quantitative recovery (≈98 %) of **aPEG**. The rate of depolymerization can be controlled by the temperature, amount of water, molecular weight of **aPEG**, and composition of the starting material. These last two parameters also allow one to tailor the mechanical properties of the final materials, and this was used to access soft, tough, and brittle vitrimers, respectively. The straightforward preparation and depolymerization of the **aPEG**-based **VU** vitrimers are interesting elements for the design of polymer materials with enhanced closed-loop recycling characteristics.

Introduction

Since the development of Bakelite in 1907,[1] polymers have become indispensable to our society. However, the remarkable growth of the world's plastic production is unsustainable[2] and makes it necessary to develop effective strategies for end-of-life scenarios of these materials that go beyond mechanical recycling and incineration.[3] One of the most promising new approaches to replace traditional polymers consists in the creation of polymers comprising dynamic covalent bonds, i.e., covalent linkages that can dynamically form, dissociate, or exchange with one another.[4]

Early reports on polymers featuring dynamic covalent bonds date back to the 1940s, when Green and Tobolsky postulated that disulfide cross-links are reversible, and enable non-degradative bond rearrangements and stress relaxation.[4] However, dynamic covalent chemistry, i.e., the chemistry of covalent bonds undergoing dynamic exchange, became a firmly established field only in the late 1990s/early 2000s.[5] This "supramolecular chemistry at the covalent level", as defined by Rowan and co-workers, proved to be relevant in the preparation of dynamic small molecules and macromolecules.[5] Further elaborating on the exploitation of dynamic linkages in polymer materials, Leibler et al. reported a major breakthrough with the development of vitrimers in 2011.[6] These polymeric materials contain dynamic covalent linkages that undergo chemical exchange reactions via an associative mechanism.[7] This feature allows the thermal reprocessing and recycling of polymer networks —which is otherwise only possible for thermoplastics—and it simultaneously provides the material with chemo-mechanical robustness during the material's service time, on account of the cross-linked structure—as in thermosets.[8] Leibler's seminal report leveraged esters and transesterification processes,[6] but the library of dynamic motifs (and associative exchange reactions) has significantly expanded since then, with copious reports on imines (transiminations),[9] diketoenamines and vinylogous urethanes (transaminations),[10] acetals (transacetalations),[11] thioureas (transcarbamoylations),[12] alkenes (olefin metathesis),[13] dioxaborolanes (metathesis),[7] and silyl ethers (exchanges).[14] A clear advantage of most of these materials in comparison to conventional thermosets is that they can be reprocessed or recycled several times by thermal treatment, which in principle should greatly reduce the need for virgin plastics and reduce their end-of-cycle environmental impact.[10a,b,15] However, the high temperatures necessary for the activation of the dynamic bonds can lead to some chemical degradation, which in turn impacts the physical properties and can cause unappealing discoloration after multiple reprocessing cycles. These problems can be avoided by depolymerization of the vitrimers under mild conditions, recovery of the constituents of the networks, and their subsequent repolymerization (i.e., closed-loop recycling). Previous reports have highlighted that the complete recovery of the starting monomers was not always possible, possibly due to challenging separation of the materials' components derived from the depolymerization process and the delicate interplay between kinetics and thermodynamics that often lead to non-exhaustive depolymerization processes.[5,16] Nevertheless, the illustrious examples of the

[*] Dr. Y. Ma, Dr. J. A. Berrocal, Prof. Dr. C. Weder
Adolphe Merkle Institute, University of Fribourg
Chemin des Verdiers 4, 1700 Fribourg (Switzerland)
E-mail: jose.berrocal@unifr.ch
christoph.weder@unifr.ch
Dr. Y. Ma, Prof. Dr. X. Jiang, Prof. Dr. Z. Shi
School of Chemistry and Chemical Engineering, Frontiers Science Center for Transformative Molecules, State Key Laboratory for Metal Matrix Composite Materials, Shanghai Jiao Tong University
Shanghai 200240 (P. R. China)
E-mail: zxshi@sjtu.edu.cn

closed-loop recycling of diketoenamine vitrimers from the Helms lab[10a] and the alkyl-polycyanurate thermosets reported by the Zhang group[15] show that the exhaustive depolymerization of polymer networks comprising dynamic covalent bonds is a priori feasible.

Among the numerous vitrimers reported thus far, the vinylogous urethanes (**VU**) pioneered by the Du Prez group[10b] have shown remarkable potential for applications, on account of their versatility, ease of synthesis, and high processability. Selected examples that showcase such broad applicability are **VU** materials used for 3D printing,[17] electrochemistry (as electrolytes),[18] antibacterial coatings,[19] shape memory materials,[20] and drug delivery.[21] Researchers have also rapidly developed an exquisite knowledge of the molecular-level processes of **VU**-based systems, which has been instrumental to achieve a high level of control over the vitrimeric behavior and reprocessability.[10c,22] However, to our best knowledge, investigations that tackle the closed-loop recycling of this rapidly growing class of vitrimers are lacking. With this in mind, we set out to create **VU** vitrimers that can be completely depolymerized in the presence of water and at ambient temperature. Although polymers that depolymerize/degrade upon exposure to neutral water might not have broad applicability, the materials selected for this study represent an ideal testbed to investigate fundamental aspects, and we hope the data will catalyze the further development of novel and technologically relevant vitrimers with closed-loop recycling capability.

Our materials design concept builds on the chemical equilibrium of the formation of **VU** from acetoacetate moieties and amines, which produces water as byproduct (Scheme 1). Following the Le Chatelier principle, it should consequently be possible to depolymerize **VU** vitrimers into the parent monomers by treatment with (an excessive amount of) water. The concept is simple and chemically sound, but it has not been reflected in the literature of **VU** vitrimers, perhaps because these materials often contain hydrophobic components that do not allow water to swell the polymers in sufficiently high concentration. This prevents complete depolymerization by limiting the concentration of water. We hypothesized that realizing **VU** vitrimers comprising polyethylene glycol (**PEG**) as major component, and tris(2-aminoethyl)amine (**TREN**) as cross-linker, would favor the depolymerization and closed-loop recycling of the network upon treatment with water. Here, we show that this is indeed the case and that this design approach allows one to fine-tune the thermomechanical properties and depolymerization rate of the resulting **PEG**-based **VU** networks. We first discuss the synthesis and mechanical properties of the new **VU** vitrimers, and then address the recovery of the **PEG** constituents after the depolymerization of the vitrimers. This is then followed by a demonstration of the reprocessing of the **PEG**-based **VU** networks either by heat-induced transamination processes or a water-mediated depolymerization-repolymerization scheme.

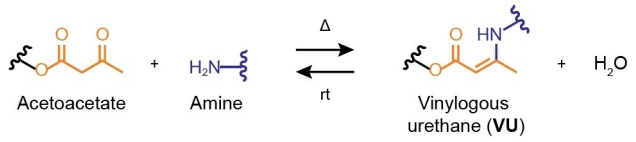

Scheme 1. Chemical equilibrium involving an acetoacetate motif and an amine, leading to the formation of a vinylogous urethane (**VU**) linkage, and water as byproduct. The formation of the **VU** bond is favored by heat and removal of water (forward reaction), while the addition of water shifts the equilibrium towards the starting materials (backward reaction).

Results and Discussion

Synthesis, Characterization, and Mechanical Properties of the Vinylogous Urethane Vitrimers

The here-investigated polymers were all based on bis(acetoacetate)-terminated poly(ethyleneglycol) building blocks (**aPEG$_x$**; Figure 1a). The subscript **x** indicates the number-average molecular weight (M_n) of the parent **PEG$_x$**. Different **aPEG$_x$** grades were prepared from commercially available, hydroxy-terminated polyethylene glycols (**PEG$_x$**) with an M_n of 1000 (**PEG$_{1k}$**), 2000 (**PEG$_{2k}$**), 3000 (**PEG$_{3k}$**), 10000 (**PEG$_{10k}$**), or 35000 (**PEG$_{35k}$**) g·mol^{-1} in transesterification reactions with *tert*-butyl acetoacetate (see page S4 of the Supporting Information for details). Adapting a recently reported procedure,[18] the reactions were carried out in the presence of an excess of *tert*-butyl acetoacetate (20 eq. for **PEG$_{1k}$**, **PEG$_{2k}$**, and **PEG$_{3k}$**; 50 eq. for **PEG$_{10k}$** and **PEG$_{35k}$**). The yield of these reactions ranged from 90 % to 94 %, while the extent of end-group functionalization varied from 92 % to 100 %, as determined by the integration of the signals in the ^{1}H NMR spectra of the purified **aPEG$_x$** (Figures S1–5; calculations on page S4–5). FT-IR spectra of the **aPEG$_x$** derivatives reveal the disappearance of the broad band at 3450 cm^{-1}, which is assigned to the *–OH* end groups of the **PEG$_x$**, and the appearance of two peaks at 1716 and 1741 cm^{-1}, which are ascribed to the *C=O* stretching vibrations of the acetoacetates introduced as chain-ends of the **aPEG$_x$** (Figure S9).

Polymer networks comprising **VU** linkages (**aPEG$_x$-yTREN**) were synthesized by reacting the various **aPEG$_x$** with tris(2-aminoethyl)amine (**TREN**). These condensation reactions involve the acetoacetate end groups of the **aPEG$_x$** and the amine functions of **TREN**; they proceed smoothly at 80 °C and afford vinylogous urethanes (**VU**s) and water as byproduct (Figure 1a). We synthesized several **aPEG$_x$-yTREN** grades by varying the M_n of **aPEG$_x$** and the molar ratio of amine to acetoacetate functional groups (**y**), which can be easily controlled by the feed of **TREN** and **aPEG$_x$** (Figure 1a; Table S1). **aPEG$_x$-yTREN** grades with **y** = 1.0 (i.e., an equimolar concentration of amine and acetoacetate groups), 1.2 (i.e., a 20 % mol excess of amines), and 1.5 (i.e., a 50 % mol excess of amines) were explored (Figure 1a; Table S1). **aPEG$_x$-yTREN** films were prepared by mixing **aPEG$_x$** and **TREN** in DMF, casting the resulting solutions into Teflon molds, heating the mixtures overnight to 80 °C, and subsequently vacuum drying the resulting films for 12 h

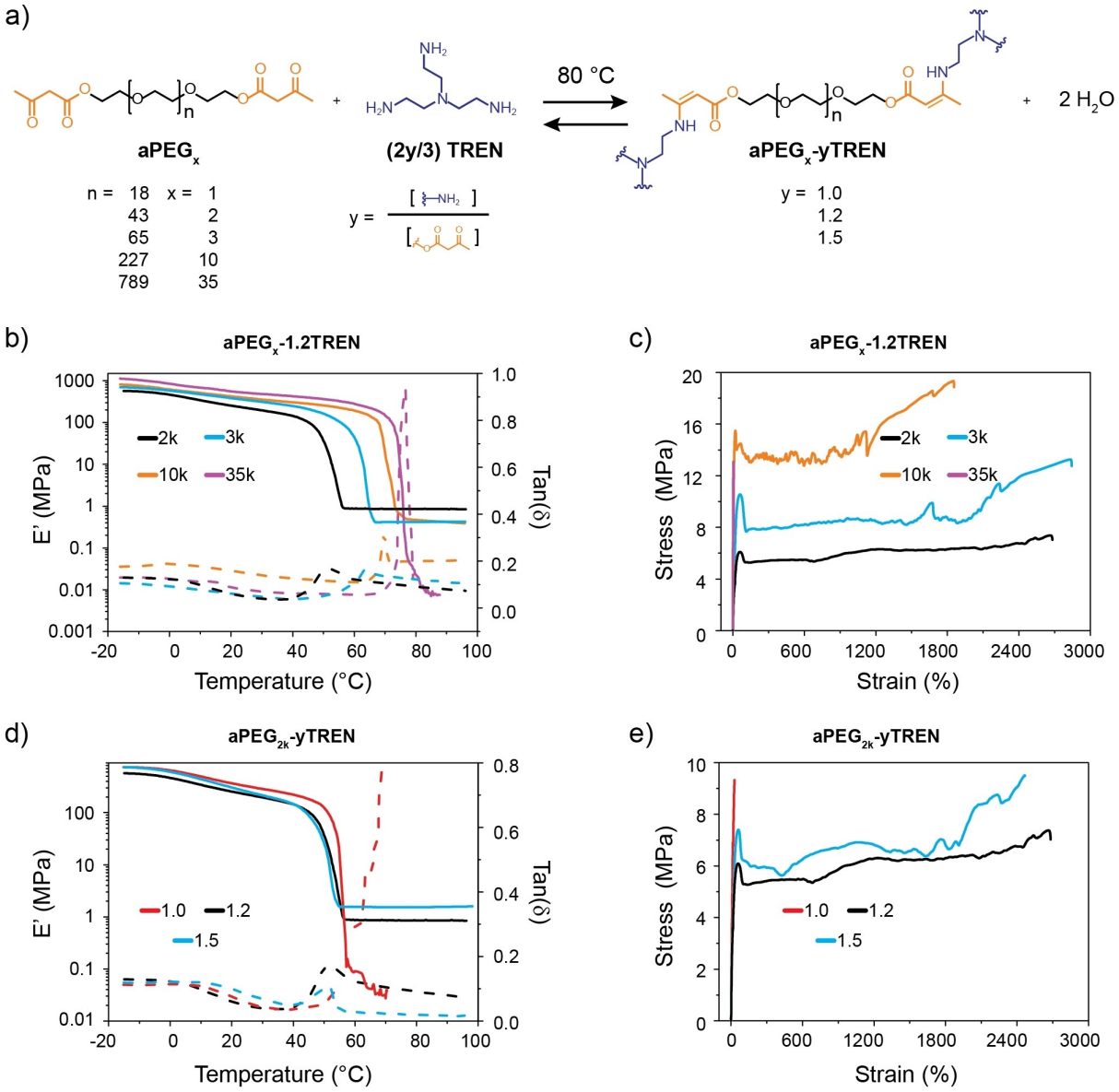

Figure 1. (a) Synthesis of **aPEG$_x$-yTREN** by the reaction of bis(acetoacetate)-terminated poly(ethyleneglycol) (**aPEG$_x$**) and tris(2-aminoethyl) amine (**TREN**). Parameters **x** and **y** indicate the number-average molecular weight (M_n) of the **PEG$_x$** segment in 1000 g·mol^{-1} and the molar ratio of amine to acetoacetate functional groups, respectively. (b,d) DMA traces showing the storage modulus (E') (solid lines) and tan δ (dashed lines) of (b) the **aPEG$_x$-1.2TREN** series and (d) the **aPEG$_{2k}$-yTREN** series as a function of temperature. (c,e) Stress-strain curves of (c) the **aPEG$_x$-1.2TREN** series and (e) the **aPEG$_{2k}$-yTREN** series.

at 80 °C (details on page S9). The materials thus prepared were analyzed by FT-IR spectroscopy, which reveals the disappearance of the acetoacetates peaks at 1716 and 1741 cm^{-1}, and the appearance of two new vibrational bands at 1604 and 1648 cm^{-1} (Figures S9, S10b), which indicate the formation of the vinylogous urethane bonds.[10b,18] The intensity of these new signals decreases (at constant **y**) as the M_n of **aPEG$_x$** is increased, reflecting that the cross-link density is reduced (Figure S10b). We also investigated the swelling ratio and gel fraction of the **aPEG$_x$-yTREN** networks by immersing the films in DMF (Figure S11), in which both **aPEG$_x$** and **TREN** are readily soluble. Within the **aPEG$_x$-1.2TREN** series, the swelling ratio increases from 500 % to 1520 %, and the gel fraction decreases from 94 % to 66 %, as the M_n of **aPEG$_x$** is increased from 1 to 10 kg·mol^{-1} (Figure S11a). Increasing the feed of **TREN** (i.e., a higher **y** value) and keeping **aPEG$_x$** the same causes a slight decrease of the swelling ratio, while the gel fraction remains practically the same (Figure S11b). These results reflect that the parameters **x** and **y** allow one to control the cross-link density and thereby the swelling characteristics of the **aPEG$_x$-yTREN** networks. **aPEG$_{2k}$-1.0TREN** and **aPEG$_{35k}$-1.2TREN** fully dissolved in DMF, suggesting that a very low **TREN** feed or a very high M_n of **aPEG$_x$** prevents the formation of cross-linked networks.

The thermal properties of the various **PEG$_x$**, **aPEG$_x$**, and **aPEG$_x$-yTREN** networks were studied by differential scanning calorimetry (DSC) (Figure S12). The DSC heating traces of all polymers, except **aPEG$_{1k}$-1.2TREN**, show endothermic peaks at temperatures between 38 and 61 °C, which are associated with the melting of crystalline domains formed by the **PEG** segments.[22] The melting temperature (T_m) increases with the M_n of **aPEG$_x$** (Table S2). For any given value of **x**, the T_m, and degree of crystallization (χ_c) decrease in the order of **PEG** > **aPEG$_x$** > **aPEG$_x$-yTREN** (Figures S12a–e, Table S2). For instance, the T_m, and χ_c values of **PEG$_{2k}$**, **aPEG$_{2k}$**, and **aPEG$_{2k}$-1.2TREN** are 52 °C and 83 %, 41 °C and 70 %, and 38 °C and 38 %, while **aPEG$_{1k}$-1.2TREN** is fully amorphous. The enthalpy of crystallization (ΔH_c) shows the same trend (Table S2). Similar behavior was observed for the other **aPEG$_x$-yTREN** series investigated (Figures S12a–e). Increasing the **y** value resulted in a small decrease of T_m, χ_c, and ΔH_c, as exemplified by the data for the **aPEG$_{2k}$-yTREN** series in Table S2, in which the T_m, χ_c, and ΔH_c dropped from 39 °C, 41 %, and 81 J·g^{-1} (**y** = 1.0), to 38 °C, 38 %, and 74 J·g^{-1} (**y** = 1.2), and 35 °C, 34 %, and 69 J·g^{-1} (**y** = 1.5).

We next studied the thermomechanical properties of **aPEG$_x$-yTREN** films by means of dynamic mechanical analysis (DMA) (Figures 1b, 1d). All DMA traces of **aPEG$_x$-1.2TREN** (**x** ≥ 2k) feature a slanted plateau regime in which the storage modulus E' adopts values between 1110 and 570 MPa. A gradual reduction of E' with temperature can be observed, and the E' trace shifts to higher values as the M_n and χ_c are increased. The DMA traces all show a sharp drop of E' at a temperature that marks the melting of the crystalline **PEG** domains. The corresponding maxima of the tan delta (tan(δ)) plots are in good agreement with the melting temperatures observed by DSC (see above). In the case of **aPEG$_2$-1.2TREN**, **aPEG$_3$-1.2TREN**, and **aPEG$_{10}$-1.2TREN**, the DMA traces show a rubbery plateau, confirming the formation of cross-linked architectures. In this regime, **aPEG$_{2k}$-1.2TREN**, which features the highest cross-link density, displays the highest E', whereas no differences can be observed for **aPEG$_{3k}$-1.2TREN**, and **aPEG$_{10k}$-1.2TREN**. By contrast, **aPEG$_{35k}$-1.2TREN** fails upon melting, reflecting that the cross-link density in this material is very low. The DMA trace of **aPEG$_{1k}$-1.2TREN** shows no obvious thermal transitions in the temperature range explored (−20 °C to 100 °C; Figure S13a), consistent with the absence of crystalline **PEG** domains, as evidenced by DSC data (Figure S12a). Figure 1d, which shows the DMA traces of the **aPEG$_{2k}$-yTREN** series, confirms that changing the **TREN** content has only a minor effect on T_m, as reflected by the DSC data. However, a pronounced effect is observed above T_m, where the increased cross-link density bestows **aPEG$_{2k}$-1.5TREN** with a higher E' (1.5 MPa) than **aPEG$_{2k}$-1.2TREN** (0.9 MPa), and the absence of cross-links causes **aPEG$_{2k}$-1.0TREN** to fail upon reaching T_m.

The mechanical properties of films of the **aPEG$_x$-1.2TREN** series were further investigated by tensile testing (Figure 1c; Figure S14, Table S3). The stress-strain curves of **aPEG$_{2k}$-1.2TREN**, **aPEG$_{3k}$-1.2TREN**, and **aPEG$_{10k}$-1.2TREN** all display the typical behavior of semicrystalline polymers, with an initial elastic regime, yield points at 30–90 % strain, and yielding deformation with modest or no strain hardening (Figure S14b). The yield stress and stress at break increase with the M_n of **aPEG$_x$** from 6.1 MPa and 7.0 MPa for **aPEG$_{2k}$-1.2TREN** to 15.5 MPa and 19.3 MPa for **aPEG$_{10k}$-1.2TREN**, and all three polymers show plastic deformation with a strain at break of more than 1800 % (Figure 1c; Table S3; Supplementary Video S1). In stark contrast, **aPEG$_{1k}$-1.2TREN**, in which the **PEG** segments do not crystallize, is an elastic material and displays much lower stress (0.9 MPa) and strain at break (98 %) values (Figure S13b). On the other hand, **aPEG$_{35k}$-1.2TREN** is highly crystalline and shows brittle failure at a maximum stress of 7.5 MPa and low strain at break (7.5 %). The influence of the **TREN** content on the tensile properties is evident from the data shown in Figure 1e. **aPEG$_{2k}$-1.5TREN** displays tensile properties that are very similar to those of **aPEG$_{2k}$-1.2TREN**, but the increased cross-link density leads to a higher stress at break (Figure 1e; Figure S15, Table S4). Somewhat surprisingly, **aPEG$_{2k}$-1.0TREN** shows brittle failure at a strain of 30 % and a stress of 9.3 MPa, which is higher than the yield stress observed for **aPEG$_{2k}$-1.2TREN** and **aPEG$_{2k}$-1.5TREN** (Figure S15b). We speculate that the low strain and high stress at break for **aPEG$_{2k}$-1.0TREN** can be attributed to the low cross-link density induced by the low **TREN** feed in the synthesis and the high χ_c, respectively (Table S2).

Next, we tested the stability of the **aPEG$_x$-yTREN** materials to oxidative conditions (for amino groups, i.e., high T and presence of air). Films of **aPEG$_{10k}$-1.2TREN** were placed in an oven at 80 °C with constant air flow for 2 days. The **aPEG$_{10k}$-1.2TREN** films thus treated were then subjected to tensile tests. The stress-strain curves recorded reveal a slight reduction in both stress and strain at break (21.1 MPa, 1180 %) compared to the original **aPEG$_{10k}$-1.2TREN** (24.0 MPa, 1380 %) (Figure S16), which we attribute to the oxidation of (some) amino groups present in the material.

Because the **aPEG$_x$-yTREN** VUs are based on hydrophilic PEG building blocks, their mechanical properties can be expected to depend on the relative humidity (RH) of the environment. To explore this, films of **aPEG$_{1k}$-1.2TREN** and **aPEG$_{10k}$-1.2TREN** were conditioned at 85 % RH for either 1 or 3 days. Subsequent tensile tests (Figure S17) show that the properties of **aPEG$_{10k}$-1.2TREN** are hardly affected, whereas the stress and strain at break of **aPEG$_{1k}$-1.2TREN** films drop from 0.9 MPa and 98 % to 0.6 MPa and 43 % after 1 day at 85 % RH and to 0.4 MPa and 29 % after 3 days at 85 % RH (Figure S17a). The different susceptibility to humidity is attributed to the crystalline nature of **aPEG$_{10k}$-1.2TREN** (Figure S12d), which limits the uptake of moisture.[23]

Since responsiveness to moisture is normally not a desirable feature in polymeric materials, we also investigated **aPTHF$_{2k}$-1.2TREN** (Figure 2), which is based on a hydrophobic building block made by end-capping poly(tetrahydrofuran) with an M_n of 2000 g·mol^{-1} with bisacetoacetate (**aPTHF$_{2k}$**) and **TREN** (synthetic details on pages S5 and S10) to understand whether the moisture

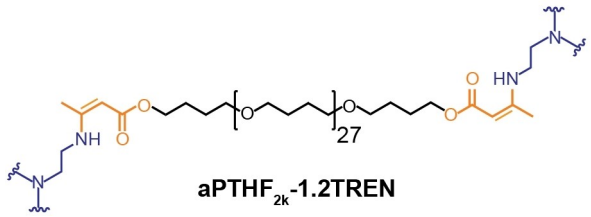

Figure 2. Chemical structure of **aPTHF$_{2k}$-1.2TREN**.

sensitivity could be suppressed. Gratifyingly, **aPTHF$_{2k}$-1.2TREN** exhibits excellent stability in the presence of various organic solvents (such as THF, $CHCl_3$, ethanol, DMF, and hexane), water, THF/H_2O mixtures, and aqueous NaOH after 3 days at room temperature (Figure S18). More importantly, the mechanical properties of **aPTHF$_{2k}$-1.2TREN** show no appreciable changes after 1 or 3 days of exposure to 85 % RH (Figure S19). Thus, the data show clearly that moisture sensitivity can be controlled via the crystallizability and polarity of the **VU**-terminated building block.

Depolymerization and Recovery of the Monomers

As reflected by Figure 1a, the formation of vinylogous urethanes is a reversible process in which the position of the equilibrium can be shifted by the addition or removal of water. To test if the addition of water would lead to depolymerization of the **VU**-based polymers, we first investigated the hydrolysis of vinylogous urethane bonds using bis-(butyl vinylogous urethane)-terminated **PEG** (**aPEG$_{2k}$-Btl**; Figure 3a), a model compound made by reacting **aPEG$_{2k}$** and butylamine (**Btl**; page S19). The conversion of **aPEG$_{2k}$-Btl** into **aPEG$_{2k}$** and **Btl** was carried out by immersing 20 mg of **aPEG$_{2k}$-Btl** in 700 µL of deuterated water (D_2O) at 25 °C, 40 °C, and 60 °C (Figure 3a), and the progress of the reactions was monitored by following the evolution of the ^{1}H NMR signals assigned in Figure 3a over time (Figure 3b; Figures S21b–d). Integration of the ^{1}H NMR signals allowed us to quantify the degree of hydrolysis (Figure S21e). At 25 °C, the extent of hydrolysis of **aPEG$_{2k}$-Btl** was ≈13 % after 30 min, increased to ≈36 % after 120 min, and reached a value of ≈88 % after 9 h (Figure 3b). When the reaction was carried out at 60 °C, ca. 93 % of **aPEG$_{2k}$-Btl** were hydrolyzed within 1 h. Monitoring the consumption of **aPEG$_{2k}$-Btl** in the presence of a large excess of D_2O as a function of time and temperature (Figure S21e) allowed us to determine the pseudo-first-order kinetic rate constants (k) of the reaction (Figure S23, Table S5). An Arrhenius plot of ln(k) against 1/T affords an activation energy (E_a) of 61 kJ mol^{-1} for the process (Figure 3c).

We also investigated the influence of the water content on the hydrolysis of **aPEG$_{2k}$-Btl** by mixing 20 mg of **aPEG$_{2k}$-Btl** and different volumes of D_2O (200, 300, 500, 700 µL) at 25 °C (Figure S22a). The extent of hydrolysis was monitored by analyzing the ^{1}H NMR signals (Figures S22b–f). As the amount of D_2O was increased from 200 to 700 µL, the extent of hydrolysis for **aPEG$_{2k}$-Btl** increased from 17 % to 36 % after 120 min, and from 76 % to 88 % after 9 h (Figure S22f). The results suggest that a large excess of D_2O is required besides high temperature to drive the hydrolysis process in **VU**-based vitrimers containing hydrophilic components.

Next, we studied the hydrolysis of **aPEG$_{2k}$-1.2TREN** in H_2O by immersing **aPEG$_{2k}$-1.2TREN** films in a ten-fold amount (in weight) of neutral H_2O at 25 °C (Figure 3d). The polymer initially swells and then gradually dissolves over time (Figure S24a). The pH value of the water phase increases from ca. 8.4 to 9.5 over the course of 2.5 hours, which reflects an increasing concentration of free amines (Figure S24b). The increase in pH is accompanied by a progressive dissolution of the polymer, which is consistent with the hydrolysis of the **VU** linkages in the polymer network. We carried out kinetic measurements for the hydrolysis of **aPEG$_{2k}$-1.2TREN** at temperatures between 20 and 80 °C in D_2O (further details in the Supporting Information on page S25). The progress of these reactions was again monitored by ^{1}H NMR spectroscopy, and the integration of the signals was used to establish kinetic profiles for these processes (Figure 3e; ^{1}H NMR spectra are shown in Figure S25). Note that the NMR technique only allows the detection of species produced by the hydrolysis that are soluble in D_2O, while the initial **aPEG$_{2k}$-1.2TREN** is NMR-silent due to its cross-linked nature. Thus, the extent of depolymerization was determined by the relative depolymerization degree (**RDD**), in which $\boldsymbol{m_t}$ is the ratio of the integrals of signal ***m*** (ascribed to the **PEG** backbone of **aPEG$_{2k}$**, see Figure 3d) and ***n*** (assigned to water in the NMR spectra of Figure S25) at time t, and $\boldsymbol{m_0}$ is the initial ratio of the integrals of signals ***m*** and ***n*** in the ^{1}H NMR spectra of the mixtures (Eq. 1).

$$\textbf{RDD}\ (\%) = (\boldsymbol{m_t} - \boldsymbol{m_0})/\boldsymbol{m_0} \qquad (1)$$

A comparison of the **RDD** determined at different temperatures (Figure 3e) shows that, also in this case, higher temperatures result in faster hydrolysis, mirroring the trend observed for **aPEG$_{2k}$-Btl**. For instance, the **RDD** is 24 % after 42 minutes at 20 °C, while it increases to 57 % after 15 min at 80 °C (Figure 3e).

We further investigated how the composition of **aPEG$_x$-yTREN** influences the water-promoted depolymerization. The first set of experiments was conducted with the **aPEG$_x$-1.2TREN** series at room temperature (page S27). All of the **aPEG$_x$-1.2TREN**/H_2O mixtures (1:15 wt:wt) were initially heterogeneous, and eventually turned into clear solutions (Figure S28). We also investigated the influence of the **TREN** feed on the depolymerization of **aPEG$_{2k}$-yTREN**, and the comparison shows that the time to full dissolution increases with the **TREN** content. The data suggest that the kinetics of the water-assisted depolymerization of the **aPEG$_x$-yTREN** can be engineered to occur within a broad time range (Figure S29), although we emphasize that the experiments reported here ultimately probe the *dissolution* and not the complete *depolymerization* of the **VU** networks.

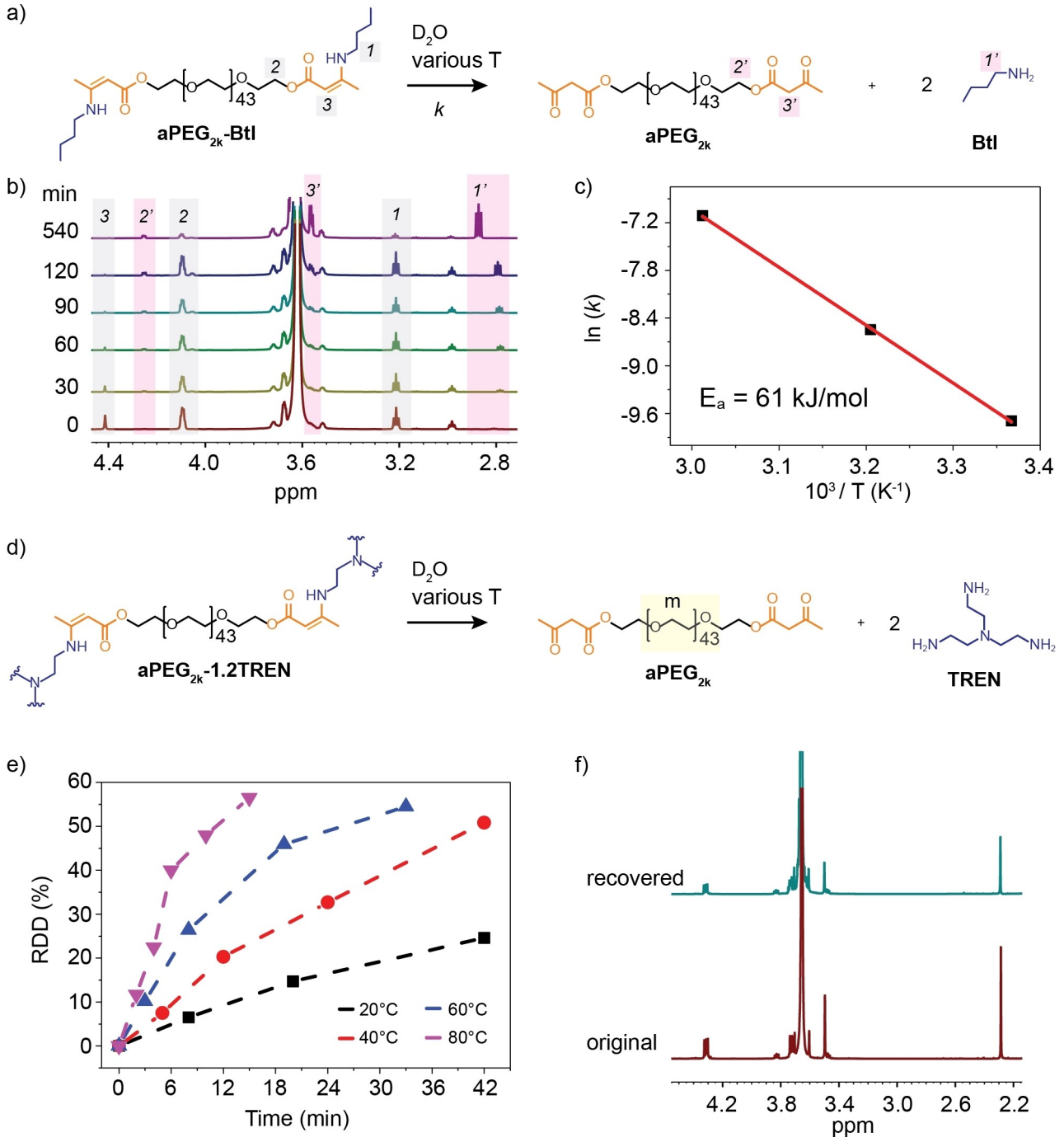

Figure 3. (a) The hydrolysis of **aPEG$_{2k}$-BtI** into **aPEG$_{2k}$** and **BtI**; this reaction was carried out in D_2O and at different temperatures. (b) Partial ^1H NMR spectra recorded during the hydrolysis of **aPEG$_{2k}$-BtI** at 25 °C; samples were taken at the times indicated. The signals used for the integration are assigned in Figure 3a. (c) Arrhenius plot for the hydrolysis of **aPEG$_{2k}$-BtI** using an excess of D_2O; the analysis affords an activation energy (E_a) of 61 kJ mol^{-1}. (d) Scheme showing the hydrolysis of **aPEG$_{2k}$-1.2TREN** into **aPEG$_{2k}$** and **TREN**; this reaction was carried out in D_2O and at different temperatures. The yellow box highlights protons *m* used for the determination of the relative depolymerization degree (**RDD**) in the ^1H NMR experiments. (e) **RDD** for the depolymerization of **aPEG$_{2k}$-1.2TREN** under formation of **aPEG$_{2k}$** and **TREN** as a function of time at 20 °C, 40 °C, 60 °C, and 80 °C in 0.55 mL of D_2O. The dashed lines are guides to the eye. (f) Comparison of the ^1H NMR spectra of original **aPEG$_{2k}$** and **aPEG$_{2k}$** recovered from the hydrolysis of **aPEG$_{2k}$-1.2TREN**.

We next pursued the recovery of **aPEG$_x$** (**x** < 35 k) or **aPTHF$_{2k}$** (Figures S26–28). Our strategy to separate **aPEG$_x$** (**x** ≤ 35k) and **TREN** was inspired by previous work from the Helms lab[10a] and leveraged the difference in the chemical properties of these two components (page S30). In order to remove **TREN**, the clear solutions produced by depolymerization for 24 h at room temperature in water (conditions discussed above) were treated with a strongly

acidic ion exchange resin, which was subsequently filtered off. Evaporation of the solvent (H_2O) from the filtrate afforded **aPEG$_x$** in a yield of 97 %–99 % (page S27). The low amounts of **TREN** used in the preparation of the **VU** vitrimers (<150 mg; Table S1) made the quantitative recovery of this component particularly challenging. Thus, to show the feasibility of the applied procedure, we carried out a model experiment in which the acidic ion exchange resin was impregnated with 0.5 g of **TREN** and further treated with an excess of trimethylamine. Filtration of the thus treated resins afforded the recovery of **TREN** in a yield of 88 % (Figure S27). The purity of the recovered **aPEG$_x$** and **TREN** was assessed by ^{1}H NMR spectroscopy, which confirmed the chemical structures and suggested the absence of (detectable) impurities (Figure 3f; S30–35).

As discussed above, **aPTHF$_{2k}$-1.2TREN** remains mechanically stable in neutral or basic water, even after being immersed for 3 days, and therefore this hydrophobic **VU** vitrimer requires different depolymerization conditions than **aPEG$_x$-yTREN**. Gratifyingly, **aPTHF$_{2k}$-1.2TREN** could be degraded by treatment with a 1 M HCl aqueous solution at room temperature. The degradation process occurred within 3 days, after which the initially clear liquid phase had turned into an off-white slurry. Extraction with $CHCl_3$, neutralization of the organic phase through washing with water, and removal of the solvent allowed the recovery of **aPTHF$_{2k}$** in high yield (95 %, page S28) and in high purity (Figure S26b).

We explored the recyclability of a (nano)filler-reinforced composite material that was prepared by combining multiwalled carbon nanotubes (**MCNs**) with **aPEG$_{10k}$-1.2TREN** (**aPEG$_{10k}$-1.2TREN/MCNs**) (synthesis on page S38). Immersing **aPEG$_{10k}$-1.2TREN/MCNs** in H_2O for 24 h afforded a suspension, from which the **MCNs** could be filtered off, leaving a clear solution containing **aPEG$_{10k}$** and **TREN** (Figure S36). Further treatment with the acidic ion exchange resin permitted the almost quantitative recovery (96 % of the initial mass) of **aPEG$_{10k}$** (Figure S36). Scanning electron microscopy (SEM) imaging and Raman spectroscopy provided qualitative indications of the unperturbed morphology of the recovered **MCNs** (Figure S37).

Finally, we tested the possibility to apply the depolymerization/separation sequence to VU networks in complex mixtures that simulated a mixed waste stream (Figure S38). The experiment was conducted by mixing **aPEG$_{10k}$-1.2TREN** with household waste (polyethylene, polypropylene, aluminum foil, tree bark, and leaves) or commodity polymer waste (polyvinyl chloride, polyethylene terephthalate, polycarbonate, and polystyrene). The mixtures were treated with water (1500 weight %) for 24 h at room temperature, and the solid components were removed via filtration. After treatment of the obtained solutions with the acidic ion exchange resin, filtration, and water evaporation, **aPEG$_{10k}$** was recovered with a negligible loss (ca. 97 % of material recovered) and in high purity, as confirmed by its ^{1}H NMR spectrum (Figures S38–39).

Thermal Reprocessing and Water-Assisted Recycling of the Vinylogous Urethane Vitrimers

As previously demonstrated by Du Prez et al., **VU** linkages can undergo transamination processes in the presence of auxiliary amines at sufficiently high temperature (60–150 °C) (Figure 4a, notice the exchange between the blue and green amines).[19b,20a,24] Such transamination offers two paths to recycle **VU** vitrimers. The first one involves the thermal reprocessing at 120–150 °C,[10b,c] while the second one relies on the depolymerization by treatment with monofunctional amines at 60–120 °C, followed by repolymerization with a fresh amine cross-linker.[24a,c–f] In addition to these established methods, we hypothesized that the water-mediated reversible (de)polymerization of **VU**-based polymer materials reported here could serve as a complementary reprocessing strategy. Thus, we attempted the reprocessing of the **aPEG$_{2k}$-yTREN** series by either activating the dynamic transamination process at 150 °C (Figure 4a, left), or by exploring the water-dependent depolymerization-polymerization sequence (Figure 4a, right).

The dynamic character of the transamination of the **aPEG$_x$-yTREN** systems was initially investigated in solution with model compound **aPEG$_{2k}$-Btl** and benzylamine (page S44). The two compounds were mixed in deuterated

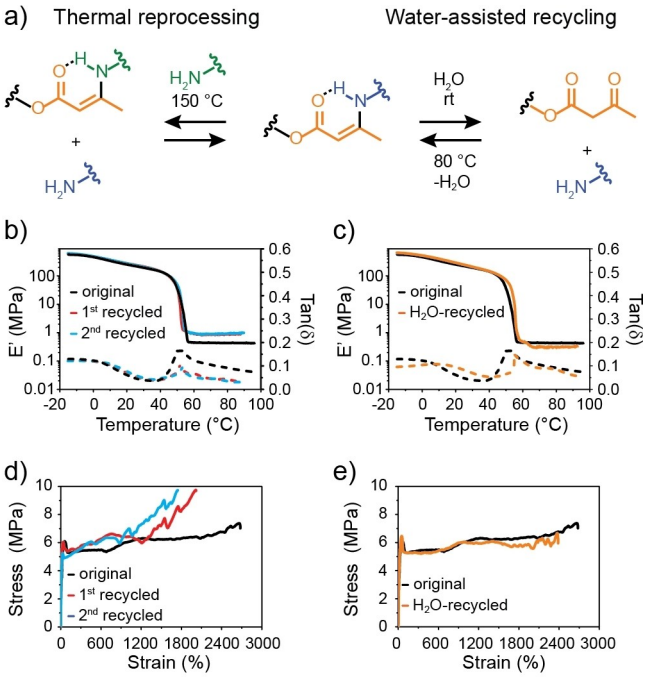

Figure 4. (a) The transamination reaction between an amine and a vinylogous urethane during thermal reprocessing (left) and the reversible, water-assisted depolymerization of a vinylogous urethane into the parent acetoacetyl- and amine-containing compounds. (b) DMA traces and (c) stress-strain curves of an as-prepared, solution-cast **aPEG$_{2k}$-1.2TREN** film, and recycled films produced by compression-molding at 150 °C (see text for details). (d) DMA traces and (e) stress-strain curves of an as-prepared, solution-cast **aPEG$_{2k}$-1.2TREN** film and a film produced by water-assisted closed-loop recycling (see text for details).

DMSO (DMSO-d_6) in a 1:6 **aPEG$_{2k}$-Btl**:benzylamine molar ratio, and the resulting mixtures were heated at 80 °C, 100 °C, and 120 °C (Figure S40). The progress of the exchange reaction was monitored by integrating the ^{1}H NMR signals of the **VU** linkages comprising the two amine substituents (Figure S40), which also allowed us to establish the kinetic profiles at each reaction temperature (Figure S41; Table S6), and determine the E_a of the transamination process, which is very low (35 kJ mol^{-1}) (Figure S42).

We then probed if the transamination process would allow the **aPEG$_{2k}$-yTREN** films to flow by performing stress relaxation experiments at different temperatures above the T_m of the **PEG** domains (Figure S43). No such experiments could be carried out for **aPEG$_{2k}$-1.0TREN**, which features a low cross-link density and flows upon melting (Figures 1d, S15). By contrast, the stress-relaxation curves of **aPEG$_{2k}$-1.2TREN** and **aPEG$_{2k}$-1.5TREN** reveal relaxations processes that we analyzed using the Maxwell model for stress-relaxation (Figures S43b, S43d, page S46). A comparison of the stress relaxation curves shows that, under the same conditions, stresses are dissipated more rapidly in **aPEG$_{2k}$-1.5TREN** than in **aPEG$_{2k}$-1.2TREN**. For instance, at 130 °C, the relaxation time (τ), at which the stress is dissipated to 1/e of its initial value, is 4.5 min for **aPEG$_{2k}$-1.5TREN** and 50 min for **aPEG$_{2k}$-1.2TREN** (Figures S43a, S43c). We attribute such difference in stress relaxation efficiency to a larger amount of free amines available in the **aPEG$_{2k}$-1.5TREN** network, which is tantamount to stating that a higher loading of free amines provides more efficient transamination processes.[10c,25] Linear fits of $\ln(\tau)$ versus $1/T$ afforded E_a values of 81.4 kJ mol^{-1} for **aPEG$_{2k}$-1.2TREN** and 127.1 kJ mol^{-1} for **aPEG$_{2k}$-1.5TREN** for the topological rearrangement, which comprises the transamination and other processes, of the polymer networks (Table S7). Moreover, by fitting the data to a Maxwell equation and assuming a Poisson's ratio of 0.5,[26] we could identify the theoretical topology-freezing temperature (T_v) (calculations on page S47, Table S7), above which the exchange reaction in the polymer material becomes active. The T_v of **aPEG$_{2k}$-1.2TREN** is 66 °C, while a value of 40 °C was determined for **aPEG$_{2k}$-1.5TREN**.

We next investigated the possibility to thermally reprocess **aPEG$_{2k}$-1.2TREN**. A film of **aPEG$_{2k}$-1.2TREN** was cut into small pieces, which were then compression-molded at 150 °C and a pressure of 10 MPa for 30 min. This treatment afforded a homogeneous film (Figure S44). The process was repeated and the mechanical properties of the original **aPEG$_{2k}$-1.2TREN** film and the samples made in the first and second recycling step were compared by DMA (Figure 4b) and tensile testing (Figure 4c). Gratifyingly, the mechanical properties of the three samples are almost indistinguishable. The DMA traces of the thermally recycled **aPEG$_{2k}$-1.2TREN** show a slight increase of E' in the rubbery regime (0.9 MPa for the recycled *vs* 0.5 MPa for the original **aPEG$_{2k}$-1.2TREN**), whereas the tensile tests reveal an increase in the stress at break (9.7 MPa for the recycled *vs* 7.0 MPa for the original **aPEG$_{2k}$-1.2TREN**) and a decrease in the strain at break (2020 % for the thermally recycled *vs* 2630 % for the original **aPEG$_{2k}$-1.2TREN**). These differences might be related to some unreacted amines and acetoacetate moieties in the as-prepared material, which was produced by solution casting, which were converted into **VU** bonds via thermal reprocessing. This seems to be supported by the lack of significant differences observed in the DMA traces and stress-strain curves of the 1st and 2nd thermally recycled films (Figures 4b–c), which suggests similar network architectures and density of cross-links. The hydrolysis of the **VU** linkages upon reprocessing could be ruled out, as this would have caused a decrease in E′ due to lowering of the density of cross-links.

Finally, we conducted similar study experiments and compared the mechanical properties of the original **aPEG$_{2k}$-1.2TREN** to those of an **aPEG$_{2k}$-1.2TREN** that was produced from depolymerized matter. Briefly, we treated **aPEG$_{2k}$-1.2TREN** with a 5-fold excess of deionized H_2O at 25 °C, which caused hydrolysis of the **VU** linkages and the solubilization of **aPEG$_{2k}$** and **TREN** (Figure S28). The solution thus produced was subsequently cast into a Teflon mold, heated to 80 °C overnight, and finally dried in vacuum at 80 °C for 12 h. The DMA and stress-strain profiles obtained by measuring the original and re-synthesized (H_2O-recycled) polymer show that the two materials display practically identical mechanical properties (Figures 4d–e), demonstrating the effectiveness of water-assisted recycling of **aPEG$_{2k}$-1.2TREN**.

Conclusion

In conclusion, we have presented a case study of the closed-loop recycling behavior of vinylogous urethane vitrimers based on bis-acetoacetate terminated polyethylene glycol and tris(2-aminoethyl) amine. In stark contrast to polymers comprising bonds derived from irreversible bond-forming reactions, polymers featuring highly dynamic covalent bonds are easier to recycle, and further allow the recovery of the original monomer in high purity and efficiency with limited costs. Indeed, the vinylogous urethane vitrimers here presented allow the almost quantitative recovery of the bis-acetoacetate terminated polyethylene glycol (ca. 98 %). The depolymerization rate can be easily adjusted by judicious choice of the reaction temperature, the amount of water, the molecular weight of the bis-acetoacetate terminated polyethylene glycol, and the stoichiometric ratio of the two starting materials. These two parameters also allow to fine tune the mechanical properties of the final materials, with formulations that proved to be soft, tough, and/or brittle. The here reported vinylogous urethanes can be reprocessed multiple times by thermal processing, and by a circular depolymerization-repolymerization scheme assisted by water. While the former has already been demonstrated, the latter is a concept that, to our best knowledge, was missing in the rapidly growing literature of vinylogous urethane vitrimers.

Supporting Information

The authors have cited additional references within the Supporting Information.[27–28]

Acknowledgements

The National Natural Science Foundation of China (52073171, 51873104) is acknowledged for financial support. Y.W.M., C.W., and J.A.B. are thankful to the Adolphe Merkle Foundation for generous financial support. All authors thank the China Scholarship Council for supporting Y.W.M.'s stay at the Adolphe Merkle Institute as a visiting scholar for one year (202006230307). Open Access funding provided by Université de Fribourg.

Conflict of Interest

The authors declare no conflict of interest.

Data Availability Statement

The data that support the findings of this study are available from the corresponding author upon reasonable request.

Keywords: 1,3-Dicarbonyl Compounds · Closed-Loop Recycling · Polyethylene Glycol · Sustainable Polymers · Vinylogous Urethane Vitrimers

[1] Leo H. Baekeland, US942699 A, **1908**.
[2] Ellen Macarthur Foundation, https://ellenmacarthurfoundation.org/the-new-plastics-economy-rethinking-the-future-of-plastics**2017**.
[3] a) B. A. Abel, R. L. Snyder, G. W. Coates, *Science* **2021**, *373*, 783–789; b) A. Rahimi, J. M. García, *Nat. Chem. Rev.* **2017**, *1*, 1–11.
[4] M. S. Green, A. V. Tobolsky, *J. Chem. Phys.* **1946**, *14*, 80–92.
[5] S. J. Rowan, S. J. Cantrill, G. R. L. Cousins, J. K. M. Sanders, F. Stoddart, *Angew. Chem. Int. Ed.* **2002**, *41*, 898–952.
[6] D. Montarnal, M. Capelot, F. Tournilhac, L. Leibler, *Science* **2011**, *334*, 965–968.
[7] T. D. M. Röttger, R. van der Weegen, A. Breuillac, R. Nicolaÿ, L. Leibler, *Science* **2017**, *356*, 62–65.
[8] a) N. Zheng, Y. Xu, Q. Zhao, T. Xie, *Chem. Rev.* **2021**, *121*, 1716–1745; b) C. J. Kloxin, C. N. Bowman, *Chem. Soc. Rev.* **2013**, *42*, 7161–7173; c) G. M. Scheutz, J. J. Lessard, M. B. Sims, B. S. Sumerlin, *J. Am. Chem. Soc.* **2019**, *141*, 16181–16196.
[9] a) R. Hajj, A. Duval, S. Dhers, L. Avérous, *Macromolecules* **2020**, *53*, 3796–3805; b) K. Liang, G. Zhang, J. Zhao, L. Shi, J. Cheng, J. Zhang, *ACS Sustain. Chem. Eng.* **2021**, *9*, 5673–5683; c) P. Taynton, K. Yu, R. K. Shoemaker, Y. Jin, H. J. Qi, W. Zhang, *Adv. Mater.* **2014**, *26*, 3938–3942.
[10] a) P. R. Christensen, A. M. Scheuermann, K. E. Loeffler, B. A. Helms, *Nat. Chem.* **2019**, *11*, 442–448; b) W. Denissen, G. Rivero, R. Nicolaÿ, L. Leibler, J. M. Winne, F. E. Du Prez, *Adv. Funct. Mater.* **2015**, *25*, 2451–2457; c) W. Denissen, M. Droesbeke, R. Nicolay, L. Leibler, J. M. Winne, F. E. Du Prez, *Nat. Commun.* **2017**, *8*, 14857.
[11] a) Q. Li, S. Ma, S. Wang, W. Yuan, X. Xu, B. Wang, K. Huang, J. Zhu, *J. Mater. Chem. A* **2019**, *7*, 18039–18049; b) S. Yu, S. Wu, C. Zhang, Z. Tang, Y. Luo, B. Guo, L. Zhang, *ACS Macro Lett.* **2020**, *9*, 1143–1148.
[12] a) L. Li, X. Chen, J. M. Torkelson, *Macromolecules* **2019**, *52*, 8207–8216; b) C.-J. Fan, Z.-B. Wen, Z.-Y. Xu, Y. Xiao, D. Wu, K.-K. Yang, Y.-Z. Wang, *Macromolecules* **2020**, *53*, 4284–4293.
[13] Y. X. Lu, Z. Guan, *J. Am. Chem. Soc.* **2012**, *134*, 14226–14231.
[14] a) C. A. Tretbar, J. A. Neal, Z. Guan, *J. Am. Chem. Soc.* **2019**, *141*, 16595–16599; b) Y. Nishimura, J. Chung, H. Muradyan, Z. Guan, *J. Am. Chem. Soc.* **2017**, *139*, 14881–14884.
[15] Z. Lei, H. Chen, C. Luo, Y. Rong, Y. Hu, Y. Jin, R. Long, K. Yu, W. Zhang, *Nat. Chem.* **2022**, *14*, 1399–1404.
[16] a) Y. Xu, S. Dai, H. Zhang, L. Bi, J. Jiang, Y. Chen, *ACS Sustain. Chem. Eng.* **2021**, *9*, 16281–16290; b) C. Bao, X. Zhang, P. Yu, Q. Li, Y. Qin, Z. Xin, *J. Mater. Chem. A* **2021**, *9*, 22410–22417; c) X. Ma, H. Xu, Z. Xu, Y. Jiang, S. Chen, J. Cheng, J. Zhang, M. Miao, D. Zhang, *ACS Macro Lett.* **2021**, *10*, 1113–1118; d) J. Wu, J. Gao, Z. Guo, H. Zhang, B. Zhang, J. Hu, M. Li, *Green Chem.* **2021**, *23*, 5647–5655; e) Y. Liu, B. Wang, S. Ma, T. Yu, X. Xu, Q. Li, S. Wang, Y. Han, Z. Yu, J. Zhu, *Compos. B* **2021**, *211*, 108654; f) X. Zhang, S. Wang, Z. Jiang, Y. Li, X. Jing, *J. Am. Chem. Soc.* **2020**, *142*, 21852–21860; g) C. Cui, X. Chen, L. Ma, Q. Zhong, Z. Li, A. Mariappan, Q. Zhang, Y. Cheng, G. He, X. Chen, Z. Dong, L. An, Y. Zhang, *ACS Appl. Mater. Interfaces* **2020**, *12*, 47975–47983; h) J. Zhang, Z. Lei, S. Luo, Y. Jin, L. Qiu, W. Zhang, *ACS Appl. Nano Mater.* **2020**, *3*, 4845–4850.
[17] W. Niu, Z. Zhang, Q. Chen, P.-F. Cao, R. C. Advincula, *ACS Mater. Lett.* **2021**, *3*, 1095–1103.
[18] Y. Lin, Y. Chen, Z. Yu, Z. Huang, J.-C. Lai, J. B. H. Tok, Y. Cui, Z. Bao, *Chem. Mater.* **2022**, *34*, 2393–2399.
[19] a) Y. Zhang, L. Yuan, Q. Guan, G. Liang, A. Gu, *J. Mater. Chem. A* **2017**, *5*, 16889–16897; b) Z. Shen, Y. Wu, S. Qiu, H. Deng, R. Hou, Y. Zhu, *Prog. Org. Coat.* **2020**, *148*, 105783.
[20] a) Z. Liu, C. Zhang, Z. Shi, J. Yin, M. Tian, *Polymer* **2018**, *148*, 202–210; b) F. Chen, Q. Cheng, F. Gao, J. Zhong, L. Shen, C. Lin, Y. Lin, *Eur. Polym. J.* **2021**, *147*, 110304; c) L. Bai, J. Zheng, *Compos. Sci. Technol.* **2020**, *190*, 108062.
[21] a) S. Efstathiou, C. Ma, D. Coursari, G. Patias, L. Al-Shok, A. M. Eissa, D. M. Haddleton, *Polym. Chem.* **2022**, *13*, 2362–2374; b) C. Wang, N. Zhao, W. Yuan, *ACS Appl. Mater. Interfaces* **2020**, *12*, 9118–9131; c) F. Wang, K. Huang, Z. Xu, F. Shi, C. Chen, *Int. J. Biol. Macromol.* **2022**, *203*, 143–152; d) X. Jiang, X. Yang, B. Yang, L. Zhang, A. Lu, *Carbohydr. Polym.* **2021**, *273*, 118547.
[22] a) C. Taplan, M. Guerre, J. M. Winne, F. E. Du Prez, *Mater. Horiz.* **2020**, *7*, 104–110; b) Y. Spiesschaert, M. Guerre, I. De Baere, W. Van Paepegem, J. M. Winne, F. E. Du Prez, *Macromolecules* **2020**, *53*, 2485–2495; c) F. Van Lijsebetten, K. De Bruycker, Y. Spiesschaert, J. Winne, F. E. Du Prez, *Angew. Chem. Int. Ed.* **2022**, *134*, e202113872; d) J. O. Holloway, C. Taplan, F. E. Du Prez, *Polym. Chem.* **2022**, *13*, 2008–2018; e) F. Van Lijsebetten, K. De Bruycker, J. M. Winne, F. E. Du Prez, *ACS Macro Lett.* **2022**, *11*, 919–924.
[23] L. F. Muff, C. Weder, *Adv. Intell. Syst.* **2023**, *5*, 2200265.
[24] a) J. Zhao, Z. Zhang, L. Cheng, R. Bai, D. Zhao, Y. Wang, W. Yu, X. Yan, *J. Am. Chem. Soc.* **2022**, *144*, 872–882; b) X. Chen, T. Bai, R. Hu, B. Song, L. Lu, J. Ling, A. Qin, B. Z. Tang, *Macromolecules* **2020**, *53*, 2516–2525; c) J. J. Lessard, G. M. Scheutz, R. W. Hughes, B. S. Sumerlin, *ACS Appl. Polym. Mater.* **2020**, *2*, 3044–3048; d) J. J. Lessard, L. F. Garcia, C. P. Easterling, M. B. Sims, K. C. Bentz, S. Arencibia, D. A. Savin, B. S. Sumerlin, *Macromolecules* **2019**, *52*, 2105–2111; e) C. Ma, W. Liu, X. Zhou, J. He, Z. Wang, Z. Wang, *ACS Sustainable*

Chem. Eng. **2022**, *10*, 6775–6783; f) Y. Zhu, F. Gao, J. Zhong, L. Shen, Y. Lin, *Eur. Polym. J.* **2020**, *135*, 109865; g) F. Hajiali, S. Tajbakhsh, M. Marić, *Polymer* **2021**, *212*, 123126.
[25] T. Stukenbroeker, W. Wang, J. M. Winne, F. E. Du Prez, R. Nicolaÿ, L. Leibler, *Polym. Chem.* **2017**, *8*, 6590–6593.
[26] M. Capelot, M. M. Unterlass, F. Tournilhac, L. Leibler, *ACS Macro Lett.* **2012**, *1*, 789–792.
[27] B. Wunderlich, *Macromolecular Physics - Crystal Melting*, Academic Press, Inc, New York, NY, **1980**.
[28] Z. Liu, C. Yu, C. Zhang, Z. Shi, J. Yin, *ACS Macro Lett.* **2019**, *8*, 233–238.

Manuscript received: May 4, 2023
Accepted manuscript online: July 13, 2023
Version of record online: ■■, ■■

Research Articles

Sustainable Polymers

Y. Ma, X. Jiang, Z. Shi,* J. A. Berrocal,* C. Weder* ——— **e202306188**

Closed-Loop Recycling of Vinylogous Urethane Vitrimers

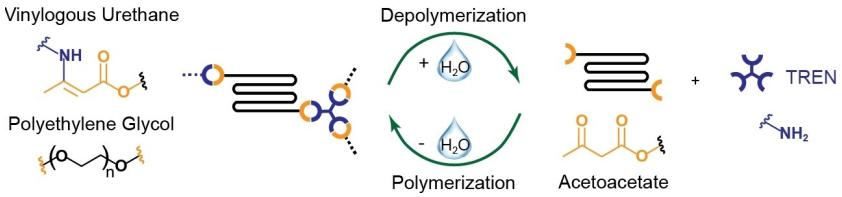

The closed-loop recycling of vinylogous urethane vitrimers made from acetoacetate-terminated polyethyleneglycol and tris(2-aminoethyl)amine is presented. Treatment with water allows the selective and quantitative recovery of the monomers, even from mixed waste streams. The modular synthetic approach allows the synthesis of materials that cover a broad range of mechanical properties and that are easy to reprocess.